

# Lattice Regularized QCD at Finite Temperature<sup>a</sup>

Frithjof Karsch

Fakultät für Physik, Universität Bielefeld, D-33615 Bielefeld, Germany

During the first part of this review we will focus on the thermodynamics of  $SU(N)$  gauge theories at finite temperature. We will present results from a calculation of electric and magnetic screening masses for the gluons, discuss calculations of the critical temperature in units of the string tension and bulk thermodynamic quantities like the energy density and pressure. In particular, the latter calculations have now reached a stage where  $O(a^2)$  cut-off effects can be controlled systematically and an extrapolation to the continuum limit can be performed. In the second part we discuss the critical behaviour of QCD with light quarks. We analyze the chiral transition in 2-flavour QCD and present results on the temperature dependence of hadron properties.

## I. Introduction

Lattice studies of the thermodynamics of QCD have been performed since more than ten years [1]. The goal of these investigations is to understand quantitatively the behaviour of strongly interacting matter at high temperatures. In order to achieve this computer simulations of lattice regularized QCD have to be performed with parameters for the quark masses and number of flavours which are as close as possible to the values in the *real world*, ie. a world where the dynamics is controlled by two light, nearly massless quark flavours. In addition these calculations should be performed as close as possible to the continuum limit in order to minimize systematic errors resulting from the finite lattice cut-off. Numerical calculations are steadily improving in both respects. Nonetheless, given the presently available computational resources, one still has to compromise either by performing calculations in the physically interesting regime with light quarks but relatively large lattice spacings and limited statistical accuracy or by analyzing the approach to the continuum limit through high statistics calculations within the context of quenched QCD, ie. in pure  $SU(N)$  gauge theories.

Most of the results with high statistical accuracy have been obtained for pure

---

<sup>a</sup>Lectures given at the "Enrico Fermi School" on *Selected Topics in non perturbative QCD*, 27 June - 7 July, Varenna, Italy

$SU(N)$  gauge theories, which do already provide a highly non-trivial model for the thermodynamics of QCD. Many of the global features of the thermodynamics like, for instance, the rapid rise of the energy density in the plasma phase towards the high temperature ideal gas limit, have been found to be qualitatively similar in  $SU(N)$  gauge theories and QCD with light quarks. Moreover, it is well known that also the *finite cut-off effects*, which are quite large in calculations of bulk thermodynamic observables, are similar in QCD and  $SU(N)$  gauge theories. The simpler  $SU(N)$  gauge theory thus is an ideal model for the systematic investigation of discretization errors and their controlled removal in the continuum limit. We will discuss this in section II of these lectures.

The investigations of the QCD thermodynamics in the presence of light quarks, on the other hand, are not yet on the same quantitative level. The analysis of the equation of state, for instance, still suffers from large discretization errors. Another important issue in the analysis of the thermodynamics with two light quarks is to understand the role of chiral symmetry restoration at the critical temperature. As this is an infrared problem, the discretization errors do not play a central role in this case. Here the main objectives are to model the correct continuum flavour symmetry in lattice regularized QCD and to perform calculations at small enough quark masses in order to be able to observe the influence of chiral symmetry breaking/restoration on the QCD thermodynamics. We will discuss this aspect in section III of these lectures.

In this short presentation we will not be able to review systematically the formulation of lattice regularized QCD. For a more detailed discussion of the basic concepts with emphasis put on the finite temperature formulation we refer to recent reviews and references given therein [2, 3, 4].

## II Equation of State for $SU(N)$ Gauge Theories

### II.1 Screening masses and perturbation theory

Our intuitive understanding of the high temperature phase of QCD and as such also of the non-abelian  $SU(N)$  gauge theories has been guided to a large extent by perturbative calculations at high temperatures. Asymptotic freedom suggests that at very high temperatures the QCD plasma approaches an ideal gas of non-interacting quarks and gluons. This requires that the temperature dependent running coupling,  $g(T)$ , becomes small. At the same time, it is well-known that perturbative calculations are faced with severe infrared problems [5] which only can be overcome, if thermal electric and magnetic masses of order  $g(T)T$  and  $g^2(T)T$ , respectively, are generated for the gluons. Even then the perturbative expansion of the thermodynamic potential is, however, known to show quite poor convergence

properties also at temperatures which are several times as large as the critical temperature [6]. One thus may wonder to what extent the concept of magnetic and electric screening masses, in particular the arguments given for their relative ordering,  $m_e(T) \simeq O(g(T)T) > m_m(T) \simeq O(g^2(T)T)$ , are of relevance beyond perturbation theory. After all, such arguments rely on the assumption that  $g(T)$  will be small at high temperature.

A recent analysis of the gluon propagator in a  $SU(2)$  gauge theory [7], performed in Landau gauge, shows that the expected ordering of magnetic and electric screening masses indeed persists down to temperatures close to  $T_c$ , ie.  $m_e(T) > m_m(T)$ . However, it also shows that at least the leading order perturbative relations for the electric mass do not hold for temperatures at least up to  $15T_c$ . Rather than decreasing with temperature  $m_e(T)/T$  does stay constant and is quite large, i.e.  $m_e(T)/T \simeq 2.5$ . Although the magnetic mass does seem to scale like  $m_m \simeq g^2(T)T$  and is smaller than  $m_e$  above  $T_c$ , also in this case the running coupling extracted from such a scaling ansatz turns out to be large, i.e.  $g^2(2T_c) \simeq 4$ . Results from a calculation in Landau gauge [7] are shown in Figure 1.

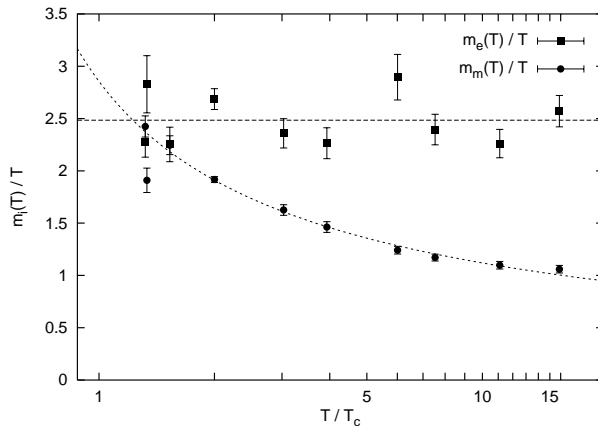


Figure 1: Electric and magnetic gluon screening masses for the  $SU(2)$  gauge theory calculated in Landau gauge [5]. For the electric mass we show a straight line fit,  $m_e = (2.484 \pm 0.052)T$ . For the magnetic mass we include the observed  $g^2$ -dependence,  $m_m = (0.466 \pm 0.015)g^2(T)T$ , with  $g^{-2}(T) = (11/12\pi^2) \ln((3.8 \pm 0.3)T/T_c)$

Although the gauge dependence of the results presented above still has to be analyzed carefully, they do suggest that the running coupling constant is larger than unity for temperatures up to a few times  $T_c$ . This observation is also in agreement with conclusions drawn from the temperature dependence of other observables like, for instance, the spatial string tension [8, 9]. One thus cannot expect that perturbation theory provides a quantitative description of bulk thermodynamics in this temperature regime [6]. A non-perturbative approach is needed.

## II.2 Cut-off dependence of thermodynamics

Lattice calculations of the energy density ( $\epsilon$ ), pressure ( $p$ ) and other thermodynamic variables led to some understanding of the temperature dependence of these quantities in the QCD plasma phase. The energy density, for instance, has been found to rise rapidly at  $T_c$  and approach the high temperature ideal gas limit from below. Such calculations are performed on finite Euclidean space-time lattices of size  $N_\sigma^3 \times N_\tau$  with non-zero lattice spacing  $a$ , which is controlled through the dimensionless coupling  $\beta = 2N/g^2$ . This fixes also the thermodynamic parameters, temperature  $T = 1/N_\tau a$  and volume  $V = (N_\sigma a)^3$ . In general such calculations suffer from two different types of finite size errors. An infra-red cut-off is introduced through the finite spatial size  $N_\sigma$  and an ultra-violet cut-off, at fixed temperature, is introduced through the temporal extent  $N_\tau$ . While  $N_\sigma$  should be large in order to reach the thermodynamic limit ( $V \rightarrow \infty$ ),  $N_\tau$  should be large in order to eliminate the influence of the regularization (finite lattice cut-off) on physical observables in the continuum limit. In the following we mainly will be concerned with the latter aspect.

As a consequence of the  $O(a^2)$  discretization errors in the standard Wilson formulation of  $SU(N)$  gauge theories thermodynamic quantities calculated on the lattice receive  $O((aT)^2)$  corrections. For an ideal gluon gas these corrections are known to be as large as 50% on lattices with  $N_\tau = 4$ , ie.  $aT \equiv N_\tau^{-1}$ . Asymptotically, in the limit  $g^2 \rightarrow 0$ , the cut-off dependence of energy density and pressure are given by [10, 11],

$$\frac{\epsilon}{T^4} = 3\frac{p}{T^4} = (N^2 - 1)\frac{\pi^2}{15} \left[ 1 + \frac{30}{63} \cdot \frac{\pi^2}{N_\tau^2} + \frac{1}{3} \cdot \frac{\pi^4}{N_\tau^4} + O\left(\frac{1}{N_\tau^6}\right) \right]. \quad (1)$$

Cut-off effects are particularly large in observables, which are sensitive to the ultra-violet behaviour of the theory. This is the case for bulk thermodynamic quantities in the high temperature limit. As will be discussed in the following these finite cut-off effects are, in fact, clearly visible in the calculations of the pressure and energy density performed on lattices with varying temporal extent, although in the temperature regime up to a few times  $T_c$  they turn out to be about a factor 2 smaller in magnitude than calculated analytically in the  $T \rightarrow \infty$  limit [12]. Only recently these calculations could be extended to lattices with sufficiently large temporal extent ( $N_\tau = 6$  and 8) that would allow an extrapolation of lattice results for bulk thermodynamic quantities to the continuum limit [10, 12].

On the other hand, cut-off effects are of less importance for the analysis of long-distance properties of the theory, such as the string tension and the deconfinement transition temperature itself. In this case it is more important to reach the large volume (thermodynamic) limit. The critical temperature is calculated at

finite lattice cut-off, ie. on lattices with fixed temporal extent  $N_\tau$ , by determining the corresponding critical couplings  $\beta_c(N_\tau)$  [12, 13, 14, 15]. A calculation of the string-tension at this value of the coupling on a large zero temperature lattice is then used to set the scale,

$$\left(\frac{T_c}{\sqrt{\sigma}}\right)_{|a\equiv 0} = \left(\frac{T_c}{\sqrt{\sigma}}\right)_{|aT=1/N_\tau} + c_2(\sigma a^2) . \quad (2)$$

A collection of results for this ratio is shown for the  $SU(2)$  and  $SU(3)$  gauge theories in Figure 2. As can be seen the  $O(a^2)$  corrections are quite small. An extrapolation to the continuum limit yields

$$\frac{T_c}{\sqrt{\sigma}} = \begin{cases} 0.69 \pm 0.01 & , \quad SU(2) \\ 0.629 \pm 0.003(+0.004) & , \quad SU(3) \end{cases} , \quad (3)$$

where the number in brackets, given in the case of  $SU(3)$ , indicates the systematic error still present in the data due to the missing extrapolation to the thermodynamic limit on the larger lattices.

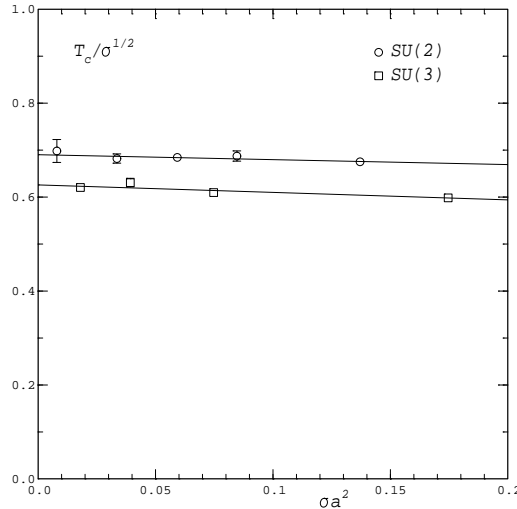


Figure 2: The critical temperature in units of the square root of the string tension for the  $SU(2)$  and  $SU(3)$  gauge theories versus the lattice cut-off squared.

Let us now turn to a discussion of bulk thermodynamic observables. The pressure can be obtained from an integration of the difference of action densities at zero ( $S_0$ ) and finite ( $S_T$ ) temperature [16],

$$\frac{p}{T^4} \Big|_{\beta_0}^\beta = N_\tau^4 \int_{\beta_0}^\beta d\beta' (S_0 - S_T) , \quad (4)$$

where the action densities themselves may be chosen appropriately in order to reduce cut-off effects. The simplest choice corresponds to the standard Wilson action, which leads to  $O((aT)^2)$  errors in thermodynamic observables. It is given in terms of plaquette expectation values,

$$S_{0(T)}^{(1\times 1)} = 6 \langle 1 - \frac{1}{3} \text{Tr} W^{(1\times 1)} \rangle_{0(T)} \quad , \quad (5)$$

with  $W^{(1\times 1)}$  denoting the product of the four link-variables around an elementary plaquette in the lattice. Various improved actions have been suggested, which reduce the cut-off effects to  $O((aT)^4)$ . One possibility is to add to the single plaquette term in the Wilson action a contribution of  $(2 \times 2)$ -loops,  $W^{(2\times 2)}$ , (for further details see [11]),

$$S_{0(T)}^{((2\times 2))} = 6 \left[ \frac{4}{3} \langle 1 - \frac{1}{3} \text{Tr} W^{(1\times 1)} \rangle_{0(T)} - \frac{1}{48} \langle 1 - \frac{1}{3} \text{Tr} W^{(2\times 2)} \rangle_{0(T)} \right] \quad . \quad (6)$$

Using either of these actions in the simulation one can perform the numerical integration defined in Eq. 4. This yields the pressure difference between two temperatures, corresponding to the two couplings  $\beta_0$  and  $\beta$ . The lower temperature, corresponding to  $\beta_0$ , can be chosen small enough so that the pressure can be approximated by zero at this point. As the low temperature phase in a  $SU(N)$  gauge theory is a glueball gas, ie. a system with rather heavy constituents, the pressure drops exponentially for  $T < T_c$ . The integration therefore can be stopped rather close to  $T_c$ . Results obtained for the pressure with the standard Wilson action on lattices with temporal extent  $N_\tau = 4, 6$  and  $8$  as well as with an improved action on a  $N_\tau = 4$  lattice are shown in Figure 3. One clearly sees the expected cut-off dependence. As discussed above, it qualitatively reflects the  $N_\tau$ -dependence of the free gluon gas, which also is shown by horizontal lines in this figure. We note that the improved action calculation, performed on a lattice with only four sides in the temporal direction indeed leads to a smaller cut-off dependence than the corresponding standard Wilson action.

Making use of basic thermodynamic relations we can then evaluate the energy density in the thermodynamic limit from the trace anomaly,

$$\frac{\epsilon - 3p}{T^4} = T \frac{\partial}{\partial T} (p/T^4) = -6N_\tau^4 \left( a \frac{\partial g^{-2}}{\partial a} \right) (S_0 - S_T) \quad , \quad (7)$$

where the derivative  $a \partial g^{-2} / \partial a$  is obtained from an explicit parameterization of the dependence of the cut-off,  $a$ , on the bare coupling  $g^2$  [12]. This is shown in Figure 4.

The much slower rise of the pressure relative to the energy density results in a large peak in the trace anomaly,  $(\epsilon - 3p)/T^4$ , at  $T_{\text{peak}} \simeq 1.1T_c$ . The trace anomaly

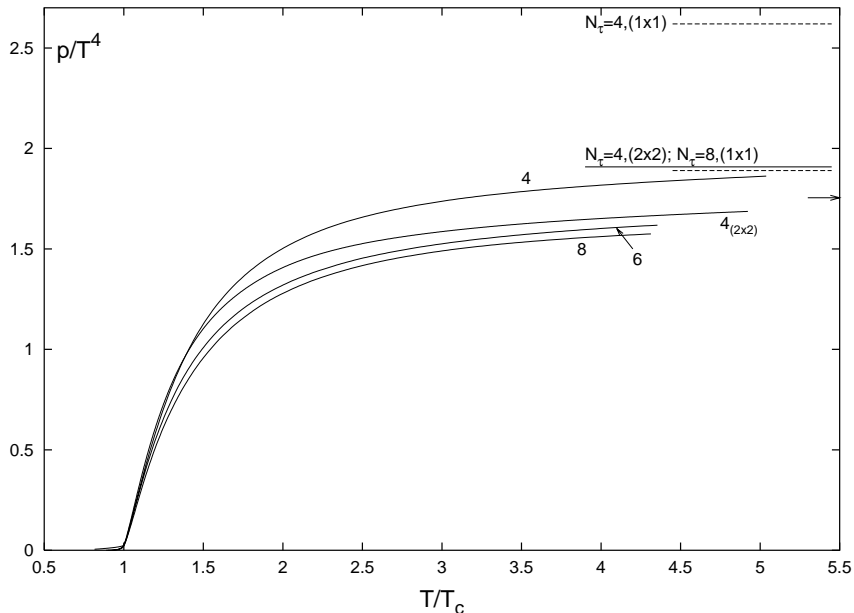


Figure 3: The pressure versus  $T/T_c$  for  $N_\tau = 4, 6$  and  $8$  obtained from an integration of the action density for the standard one-plaquette Wilson action. For  $N_\tau = 4$  we also show the result obtained with an improved action ( $4_{(2 \times 2)}$ ).

defines, the difference between the gluon condensate at zero and finite temperature  $\epsilon - 3p = G^2(0) - G^2(T)$ . From Figure 4 we find at  $T_{\text{peak}}$ ,

$$(\epsilon - 3p)_{\text{peak}} = (0.57 \pm 0.02)\sigma^2 \simeq 2.3 \text{ GeV/fm}^3, \quad (8)$$

where we have used the result given in Eq. 3 for the critical temperature in units of the string tension and  $\sqrt{\sigma} \simeq 420 \text{ MeV}$  in order to set the physical scale. This result is, in fact, compatible with conventional values for the zero temperature gluon condensate,  $G^2(0) \simeq 2 \text{ GeV/fm}^3$  [17]. It, therefore, suggests that  $G^2(T) \simeq 0$  at  $T_{\text{peak}}$ .

### II.3 Extrapolation to the continuum limit

Based on the analysis of the pressure and energy density on various size lattices one can now attempt to extrapolate these quantities to the continuum limit. At present this can only be done for the Wilson action where results do exist on lattices with temporal extent up to  $N_\tau = 8$ . Using an ansatz motivated by Eq. 1,

$$\left(\frac{p}{T^4}\right)_{N_\tau} = \left(\frac{p}{T^4}\right)_\infty + \frac{\text{const.}}{N_\tau^2}, \quad (9)$$

we extrapolate the  $N_\tau = 6$  and  $8$  data, respectively [12]. The resulting continuum predictions for the pressure, energy density and entropy density are shown in Figure 5. We generally find that the difference between the extrapolated values and the

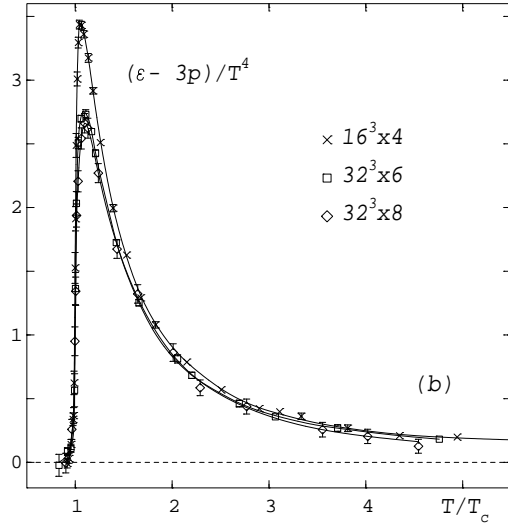


Figure 4: The difference  $(\epsilon - 3p)/T^4$  obtained from calculations with the standard Wilson action on lattices with temporal extent  $N_\tau = 4, 6$  and  $8$ .

results for  $N_\tau = 8$  is less than 4%, which should be compared with the corresponding result for the free gas, where the difference is still about 8%. This suggests that relative to the ideal gas case more low momentum modes, which are less sensitive to finite cut-off effects, contribute to thermodynamic quantities.

Knowing the energy density and pressure as a function of temperature we also can evaluate other thermodynamic quantities. A quantity of particular interest for the description of the hydrodynamic expansion of a quark-gluon plasma created in a heavy ion collision is the velocity of sound,

$$v^2 = \frac{dp}{d\epsilon} . \quad (10)$$

Already from Figure 5 it is clear that  $v^2$  will be small close to  $T_c$  because the pressure changes only little there, while the energy density rises rapidly. This, indeed, is seen in Figure 6. We also note that the velocity of sound rapidly approaches the ideal gas limit,  $v_{\text{ideal}}^2 = 1/3$ .

The above discussion of energy density and pressure in a  $SU(N)$  gauge theory has shown, that both quantities approach the ideal gas limit from below. We note that the energy density rapidly rises to about 85% of the ideal gas value at  $2T_c$  and then shows a rather slow increase, which is consistent with a logarithmic increase as one would expect if the coupling  $g(T)$  changes only logarithmically with temperature.



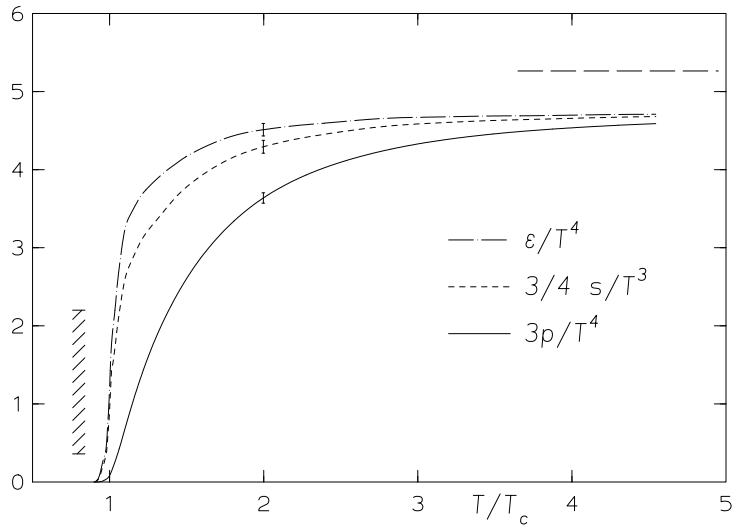


Figure 5: Extrapolation to the continuum limit for the energy density, entropy density and pressure versus  $T/T_c$ . The dashed horizontal line shows the ideal gas limit. The hatched vertical band indicates the size of the discontinuity in  $\epsilon/T^4$  (latent heat) at  $T_c$  [10]. Typical error bars are shown for all curves.

We have not discussed here the status of the equation of state for QCD with light quarks. A detailed investigation for two flavour QCD has been performed recently on lattices with temporal extent  $N_\tau = 4$  [18]. However, also here an analysis on larger lattices is still needed in order to control the obviously present large discretization errors.

### III QCD with Light Quarks

#### III.1 The chiral phase transition

A well established result from lattice calculations is the strong dependence of the order of the phase transition on the QCD symmetries related to the colour as well as the flavour degrees of freedom. In the absence of quarks, ie. in pure  $SU(N)$  gauge theories, the phase transition is second order for  $N = 2$  and first order for  $N = 3$ . In the case of QCD with  $n_f$  light quark flavours the transition is first order for  $n_f \geq 3$  and does seem to be continuous for  $n_f = 2$ . Lattice calculations also show a strong dependence of the transition temperature on the number of partonic degrees of freedom. The transition temperature, expressed for instance in units of the square root of the string tension ( $T_c/\sqrt{\sigma}$ ), is substantially smaller in QCD with light quarks than in a pure gauge theory. In the case of QCD with two light quarks one finds  $T_c(n_f = 2) \simeq 150\text{MeV}$ , while in the purely gluonic theory,  $n_f \equiv 0$ ,  $T_c$

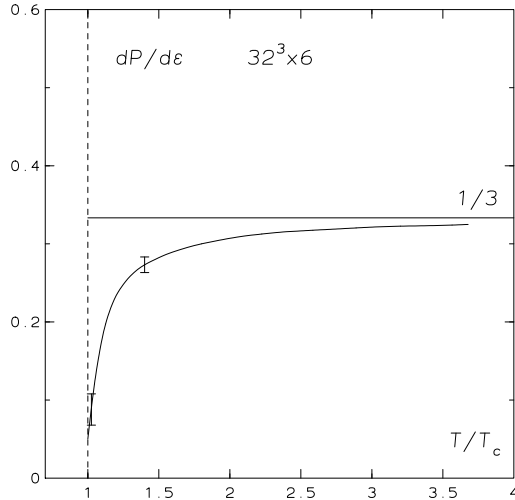


Figure 6: Velocity of sound for the  $SU(3)$  gauge theory calculated on a lattice with temporal extent  $N_\tau = 6$ . We do not observe any significant cut-off dependence for this derivative.

is found to be substantially higher,  $T_c(n_f = 0) \simeq 260\text{MeV}$ . As discussed in the previous section this may be understood in terms of a percolation threshold: In the absence of quarks there are no light hadrons, the lightest states are glueballs with a mass of  $O(1\text{ GeV})$ . Therefore, a rather high temperature is needed to excite enough of these heavy glueball states in order to reach a critical density where hadrons start overlapping.

With increasing temperature non-perturbative properties of the QCD vacuum, like confinement and chiral symmetry breaking, get modified through the thermal heat bath and eventually disappear above  $T_c$ . Non-vanishing condensates play an important role in understanding these non-perturbative features of QCD. They vary with temperature in the vicinity of the QCD phase transition. The restoration of chiral symmetry at  $T_c$  will, for instance, be reflected in a characteristic temperature dependence of the chiral condensate,  $\langle\bar{\psi}\psi\rangle \sim |T - T_c|^\beta$ , which also should have consequences for the properties of hadrons close to  $T_c$ . Effective theories, deduced from QCD in order to describe low energy properties of hadrons, establish a close link between hadronic properties and the non-perturbative structure of the QCD vacuum. This is, for instance, used in the operator product expansion (OPE) for correlation functions of hadronic currents [19], which allows to relate hadron masses to condensates of the quark and gluon fields. The temperature and density dependence of the latter has been discussed within the context of chiral perturbation theory [17].

We will discuss here some of the recent results of lattice calculations on the phase transition in two-flavour QCD as well as an analysis of hadronic properties close to the QCD phase transition. Our discussion is limited to the staggered formulation

of lattice regularized QCD. First attempts to study the chiral symmetry restoration also with Wilson fermions have been reviewed in [4]. In the next section we briefly discuss the critical behaviour in two-flavour QCD. Section III.3 is devoted to a discussion of lattice calculations of hadron masses and decay constants at finite temperature within the quenched approximation.

### III.2 The chiral transition in two-flavour QCD

The nature of the chiral phase transition does seem to depend strongly on the number of light quark flavours,  $n_f$ . The special role of two-flavour QCD has been noticed already some time ago by Pisarski and Wilczek [20]. They have suggested that the dynamics of the chiral phase transition is controlled by an effective, 3- $d$  scalar Lagrangian constructed in terms of the chiral order parameter field,  $\sigma \sim \bar{\psi}\psi$ . This effective theory has a global  $O(4)$  symmetry ( $SU(2) \times SU(2)$ ), which is spontaneously broken to  $SU(2)$ . It therefore is expected that in the case of a continuous transition the critical behaviour is governed by critical exponents of a 3- $d$ ,  $O(4)$  symmetric spin model [20, 21]. A remaining question in this scenario is to what extent the axial  $U(1)$  influences the critical behaviour in the vicinity of  $T_c$  [21, 22]. An even more fundamental problem is whether an effective scalar theory can at all describe the critical behaviour of a theory, in which the scalar fields are only constructed as fermionic bilinears. It recently has been argued by Kocić and Kogut that this may not be the case and that two-flavour QCD may instead show mean field behaviour in the vicinity of  $T_c$  [23]. In lattice calculations an additional problem arises: None of the fermion Lagrangians used for numerical calculations has the complete chiral symmetry of the continuum Lagrangian. In the staggered fermion formulation, for instance, one has a chiral  $U(1)$  rather than the full  $SU(2)$  symmetry, which only is restored in the continuum limit. This too may influence the critical behaviour in numerical studies. A detailed quantitative investigation of the critical behaviour thus is needed in different lattice formulations. Here we will restrict our discussion to the case of staggered fermions.

The critical behaviour of QCD with light quarks is controlled by two dimensionless parameters, the reduced temperature  $t = (T - T_c)/T_c$  and the scaled quark mass,  $h = m_q/T$ . The latter corresponds to an external magnetic field in spin models. In the case of QCD with dynamical quarks it is the quark mass rather than the spatial lattice volume, which is the most stringent limitation for large correlation lengths in the vicinity of the critical point. Rather than performing a finite size scaling analysis, as it has been done in the case of the deconfinement transition in  $SU(N)$  gauge theories, it thus is more appropriate to consider the scaling behaviour in terms of the quark mass. Finite volume effects may in a first approximation be ignored.

In the vicinity of the critical point the behaviour of bulk thermodynamic quan-

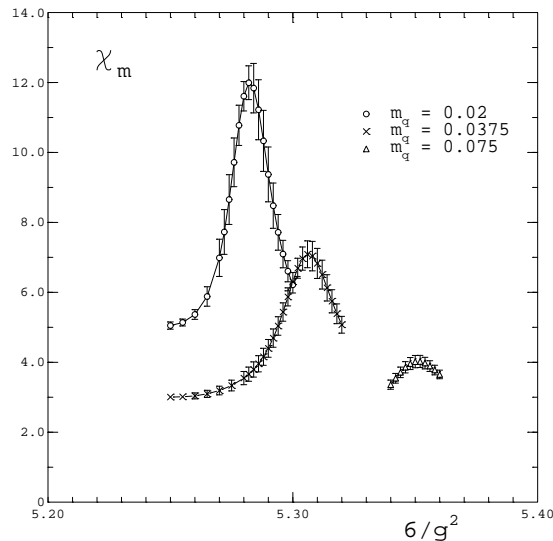


Figure 7: The chiral susceptibility in two-flavour QCD versus  $6/g^2$  for three values of the quark mass on a  $8^3 \times 4$  lattice.

tities is related to thermal ( $y_t$ ) and magnetic ( $y_h$ ) critical exponents, which characterize the scaling behaviour of the singular part of the free energy density,

$$f_s(t, h) \equiv -\frac{T}{V} \ln Z_s = b^{-1} f(b^{y_t} t, b^{y_h} h) . \quad (11)$$

Here  $b$  is an arbitrary scale factor. Various scaling relations for thermodynamic quantities can be derived from Eq. 11 [24, 25]. For instance, one finds for the chiral order parameter,  $\langle \bar{\psi} \psi \rangle$ , and its derivative with respect to the quark mass (the chiral susceptibility  $\chi_m$ )

$$\begin{aligned} \langle \bar{\psi} \psi \rangle(t, h) &= h^{1/\delta} F(z) \\ \chi_m(t, h) &= \frac{1}{\delta} h^{1/\delta-1} \left[ F(z) - \frac{z}{\beta} F'(z) \right] , \end{aligned} \quad (12)$$

with scaling functions  $F$  and  $F'$  that only depend on a specific combination of the reduced temperature and scaled quark mass,  $z = th^{-1/\beta\delta}$ . The critical exponents  $\beta$  and  $\delta$  are given in terms of  $y_t$  and  $y_h$  as  $\beta = (1 - y_h)/y_t$  and  $\delta = y_h/(1 - y_h)$ . A direct consequence of Eq. 12 is, for instance, that  $\chi_m$  has a peak located at some fixed value of  $z_c$ . This defines a pseudo-critical point,  $t_c(h) \equiv z_c h^{1/\beta\delta}$ , at which the peak height of  $\chi_m$  increases with decreasing quark mass according to Eq. 12. Fig. 7 shows the scaling behaviour of  $\chi_m$  for three values of the quark mass [25]. The rapid rise of  $\chi_m$  with decreasing quark mass can be used to determine the critical exponent  $\delta$ .

Another useful observable for the determination of the critical exponent  $\delta$  is the

chiral cumulant,

$$\Delta(z) = \frac{h\chi_m}{\langle\bar{\chi}\chi\rangle} . \quad (13)$$

From Eq. 12 it follows that  $\Delta$  is directly a scaling function, ie. it only depends on  $z$ . Moreover, it is uniquely determined at  $z = 0$ , where it takes on the value  $1/\delta$  even at non-vanishing values of the quark mass. The chiral cumulant thus allows a direct calculation of this critical exponent. In Fig. 8a we show a collection of the pseudo-critical couplings obtained from Monte Carlo calculations with various values of the quark mass and on various different lattice sizes. The curves show various fits for the quark mass dependence of these pseudo-critical couplings. Apparently it is difficult to distinguish  $O(4)$  exponents from mean field exponents in this way. We note, however, that the location of the zero quark mass critical coupling is quite well determined. The cumulant  $\Delta$  is shown in Fig. 8b. For the two smaller quark masses this quantity has been evaluated in the region of the estimated zero quark mass critical coupling,  $\beta_c(m_q = 0) \simeq 5.243(10)$ . In this interval the cumulant takes on values between 0.21 and 0.26, which is compatible with the  $O(4)$  exponent  $1/\delta = 0.205(45)$ .

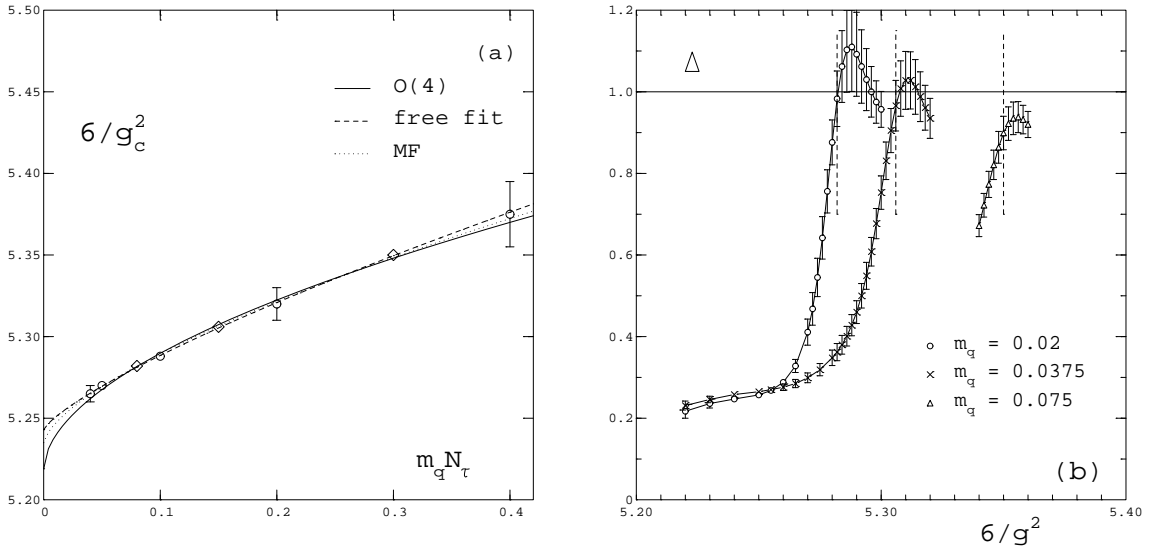


Figure 8: The pseudo-critical couplings (a) of the chiral transition in two-flavour QCD on lattices with temporal extent  $N_\tau = 4$  and the chiral cumulant (b). Shown are results from calculations with different values of the quark mass on a  $8^3 \times 4$  lattice.

Further scaling relations can be obtained by considering the quark mass dependence of the thermal susceptibility,  $\chi_t \sim \partial\langle\bar{\psi}\psi\rangle/\partial t$ , and the specific heat. A combined analysis of these allows a determination of the critical exponents  $y_t$  and  $y_h$ . Results from a first analysis of this kind [25] are summarized in Table 1 and

compared with the known exponents for 3- $d$ ,  $O(4)$  symmetric spin models [26] and mean field behaviour.

Table 1: Thermal ( $y_t$ ) and magnetic ( $y_h$ ) exponents from simulations of two-flavour QCD on an  $8^3 \times 4$  lattice (LGT). Also given are mean field exponents (MF) and those for a 3- $d$ ,  $O(4)$  symmetric spin model.

	LGT	$O(4)$	MF
$y_t$	0.69(7)	0.446(5)	0.5
$y_h$	0.83(3)	0.830(6)	0.75

As can be seen from the Table the exponent  $y_h$  extracted from lattice calculations is in very good agreement with the expected  $O(4)$  model behaviour. It corresponds to a value of 0.205(45) for the exponent  $1/\delta$ , which is significantly below the value  $1/3$  expected for a mean field critical exponent. The exponent  $y_t$ , however, comes out too large in the present calculation. It may be expected that the determination of  $y_t$  is more sensitive to finite volume effects than that of  $y_h$ . In the limit of vanishing quark masses it is  $y_t$  that controls the finite volume scaling behaviour of thermodynamic quantities.

Clearly the analysis of critical exponents on a  $8^3 \times 4$  lattice can only be considered as a first exploratory step towards a detailed investigation of critical exponents in two-flavour QCD. In the near future calculations on larger lattices with smaller quark masses will certainly lead to much better determinations of critical exponents. This should allow to distinguish between mean field and  $O(4)$  critical behaviour.

The chiral susceptibility,  $\chi_m$ , has a very narrow peak at the pseudo-critical point. This indicates that only in this region contributions from the singular part of the free energy, which is responsible for the occurrence of a phase transition, is dominant. This behaviour is consistent with the temperature dependence of  $\langle \bar{\psi}\psi \rangle$ , which leads to deviations from the zero temperature condensate only close to  $T_c$ . We thus expect that also hadronic properties will show significant modifications only in a narrow temperature regime close to  $T_c(m_q) \equiv T_{\text{peak}}$ ,

$$\left| \frac{T_{\text{peak}/2} - T_{\text{peak}}}{T_{\text{peak}}} \right| \lesssim 0.1 \quad . \quad (14)$$

### III.3 Hadronic properties close to $T_c$

Information about hadron masses and decay constants can be extracted in lattice simulations from the long-distance behaviour of correlation functions of hadron op-

erators

$$G_H(x) = \langle H(x)H^+(0) \rangle \rightarrow e^{-m_H|x|} \quad , \quad x \equiv (\tau, \vec{x}) \quad , \quad (15)$$

where  $H(x)$  denotes an operator with the appropriate quantum numbers of the hadronic state under consideration, for instance  $H(x) = \bar{\psi}_u(x)\gamma_5\psi_d(x)$  for the pion. At zero temperature one studies the behaviour of the correlation function at large Euclidean times  $\tau$ . From the exponential decay of  $G_H$  one deduces the hadron mass of the lightest state in this channel, whereas the amplitude is related to the decay constant of this hadronic state. At finite temperature the Euclidean extent is limited,  $0 \leq \tau \leq 1/T$ , and one thus studies the behaviour of  $G_H$  for large spatial separations,  $|\vec{x}| \rightarrow \infty$ . This yields information about the finite temperature screening masses which are related to pole masses as long as there is a bound state in the quantum number channel under consideration.

Finite temperature screening masses have been studied in lattice simulations of QCD for quite some time [27]. A very drastic qualitative change in the screening masses is seen when one crosses the QCD transition temperature. Parity partners become degenerate above  $T_c$ , the pseudo-scalar mass becomes massive and approaches the free quark/anti-quark value,  $m_{\text{meson}} = 2\pi T$ , at large temperatures. These features do not seem to depend much on the number of quark flavours. In particular, they also have been found in quenched QCD simulations. It thus seems to be meaningful to first study the temperature dependence of hadronic properties in the quenched approximation where results on large lattices with high accuracy can be obtained. In the following we will describe the results of such an investigation performed on a rather large lattice ( $32^3 \times 8$ ) close to the phase transition temperature [28].

### III.3.1 The GMOR relation and the pion decay constant

The GMOR relation gives the chiral condensate in terms of the pion mass and pion decay constant,

$$f_\pi^2 m_\pi^2 = m_q \langle \bar{\psi}\psi \rangle_{m_q=0} \quad . \quad (16)$$

Below  $T_c$  the pion is a Goldstone particle, its mass squared depends linearly on the quark mass,

$$m_\pi^2 = a_\pi m_q \quad . \quad (17)$$

A calculation of the chiral condensate and the pion mass at different values of the quark mass allows the determination of the pion slope,  $a_\pi$ , and the zero quark mass limit of the condensate,  $\langle \bar{\psi}\psi \rangle_{m_q=0}$ .

The pion decay constant  $f_\pi$  can be determined directly from the relevant matrix element

$$\sqrt{2}f_\pi m_\pi^2 = \langle 0 | \bar{\psi}_u \gamma_5 \psi_d | \pi^+ \rangle . \quad (18)$$

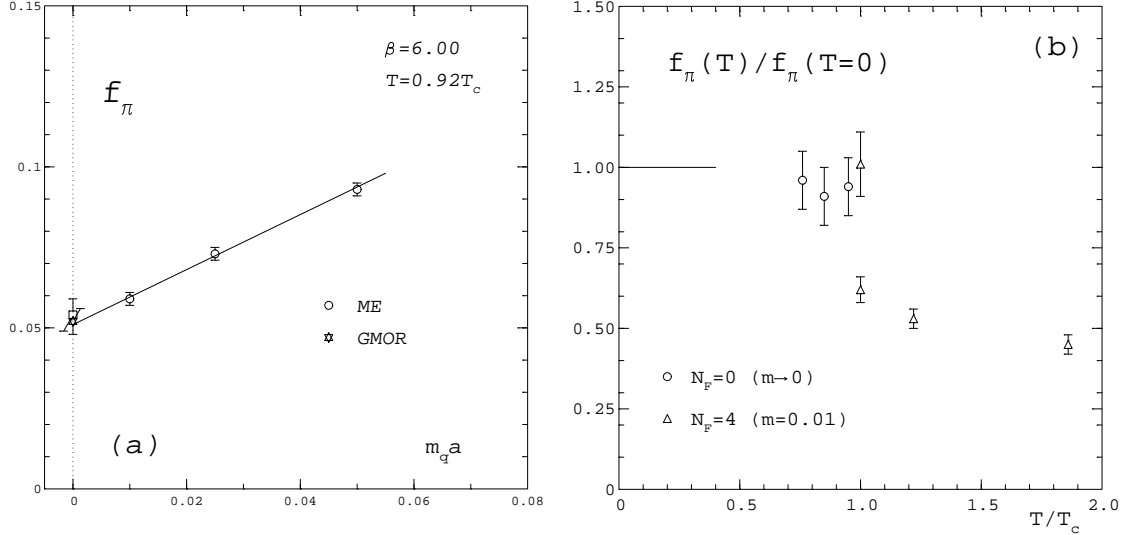


Figure 9: Test of the GMOR relation at  $T = 0.92 T_c$  in quenched QCD (a) and the temperature dependence of the pion decay constant (b). In (a) we compare the results obtained from the amplitude of the pion correlation function through Eq.(15) (circles) and extrapolated to zero quark mass with the result obtained from the GMOR relation (star, on top of the circle at  $m_q a = 0$ ). Also shown is the zero temperature result at this value of the gauge coupling (square).

The square of the matrix element appearing on the right hand side of Eq. 18 is proportional to the amplitude of the pion correlation function and can be determined in a Monte Carlo calculation. A comparison of  $f_\pi$  determined this way with the ratio  $\langle \bar{\psi}\psi \rangle_{m_q=0} / a_\pi$  thus provides a direct test of the GMOR relation at finite temperature. This is shown in Fig. 9a at  $T \simeq 0.92 T_c$ . Moreover, we can compare the value of  $f_\pi$  calculated at finite temperature with corresponding zero temperature results. This is shown in Fig. 9b. Clearly we do not have any evidence for violations of the GMOR relation nor for a significant change of  $f_\pi$  with temperature below  $T_c$ . The sudden change above  $T_c$  reflects the drastic change in the structure of the pseudo-scalar correlation function. It does no longer have a pole corresponding to a Goldstone-particle (pion). The existence of a pseudo-scalar bound state above  $T_c$  thus is questionable. Certainly for large temperatures such a state does not exist, the correlation function is dominated by a quark/anti-quark cut. The notion of  $f_\pi$  used for the square root of the amplitude of the correlation function should thus be used with caution above  $T_c$ .

### III.3.2 Vector meson mass and nucleon mass



The possibility of a variation of the  $\rho$  meson mass with temperature has been discussed a lot as this might lead to modifications of dilepton spectra, which are experimentally detectable. The temperature dependence of the meson masses has been discussed within the framework of the OPE. Arguments have been given that the meson masses are temperature independent up to  $O(T^2)$  [29]. The Monte Carlo calculations of the vector meson correlation function at finite temperature also show no significant temperature dependence of the mass even close to  $T_c$ . In Fig. 10 we show the result of our calculation of the screening mass in the vector channel correlation function at  $T \simeq 0.92T_c$  and compare this with zero temperature calculations at the same value of the gauge coupling. There is no evidence for any temperature dependence. The same holds true for the nucleon mass, although the details are more subtle in this case. As can be seen in Fig. 10b there is a clear difference between the local masses,  $m_N(z) \sim \ln G_N(z)/G_N(z+1)$ , extracted on a large zero temperature lattice and those extracted at finite temperature on a lattice of size  $32^3 \times 8$ . However, as the nucleon is a fermion, there is a non-negligible contribution from the non-zero Matsubara mode to the nucleon screening mass,

$$m_N = \sqrt{\tilde{m}_N^2 + (\pi T)^2} \quad (19)$$

After removing the thermal contribution,  $\pi T$ , the nucleon mass,  $\tilde{m}_N$ , agrees with the zero temperature result within statistical errors.

## IV. Conclusions

We have discussed recent detailed studies of the equation of state of the  $SU(3)$  gauge theory. Deviations from an ideal gas behaviour are still significant at temperatures of a few times  $T_c$ . The now existing extrapolation of the  $SU(3)$  equation of state to the continuum limit does provide a good basis for quantitative comparisons with perturbative calculations and phenomenological models [30].

The discussion of basic properties of the thermodynamics of two-flavour QCD shows that there are strong indications for a second order phase transition. However, whether two-flavour QCD is, indeed, in the same universality class as the  $3d$ ,  $O(4)$  model cannot yet be decided on the basis of the existing numerical data and needs further detailed investigations on larger lattices and with smaller quark masses.

At least up to temperatures of about  $0.9T_c$  so far no statistically significant temperature dependence could be observed for basic properties of hadrons. This is true for the chiral condensate, hadron masses as well as decay constants calculated in quenched QCD. At least for the chiral condensate one expects, however, a strong variation with temperature for  $0.9T_c < T < T_c$ , in particular in the case of a second order phase transition. This is clearly supported by the currently available lattice

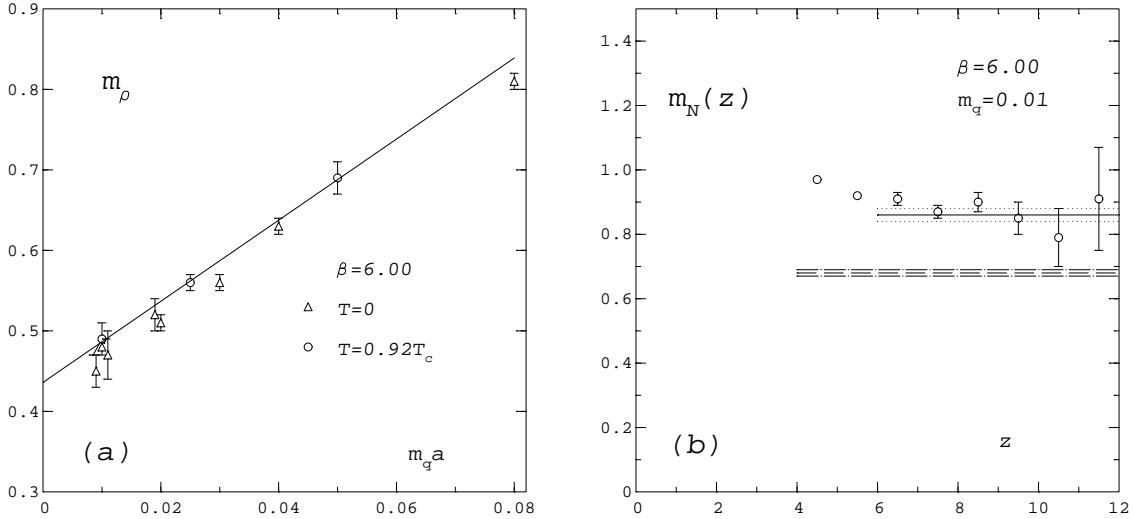


Figure 10: The  $\rho$ -meson mass in quenched QCD for various values of the quark mass (a) and local masses from the nucleon correlation function (b). The simulations have been performed at fixed value of the gauge coupling,  $6/g^2=6.0$ , on a  $32^3 \times 8$  lattice corresponding to  $T \simeq 0.92 T_c$  and on various low temperature lattices [5]. In (b) we show estimates for the nucleon mass obtained from the nucleon correlation function at distance  $z$ . These local masses converge to the nucleon mass in the limit  $z \rightarrow \infty$ . The horizontal band indicates the corresponding extrapolation at zero temperature. No temperature dependence is visible in the  $\rho$ -meson mass as well as the nucleon mass (see text for appropriate subtraction of the finite temperature Matsubara mode).

calculations in two-flavour QCD. The influence of this on the behaviour of hadronic parameters will certainly also be investigated in the near future.

## Acknowledgements

The numerical work that has been reviewed here has been performed on the Cray YMP at the HLRZ-Jülich and the QUADRICS parallel computer at the University of Bielefeld, funded by DFG under contract No. Pe 340/6-1. The work has also been supported by the Deutsche Forschungsgemeinschaft under grant Pe 340/3-2 and Pe 340/3-3.

## References

- [1] L.D. McLerran and B. Svetitsky, Phys. Lett. B98 (1981) 195;  
 J. Kuti, J. Polonyi and K. Szlachanyi, Phys. Lett. B98 (1981) 199;  
 J. Engels, F. Karsch, I. Montvay and H. Satz, Phys. Lett. B101 (1981) 89.

- [2] F. Karsch, *Simulating the Quark-Gluon Plasma on the Lattice*, Advanced Series on Directions in High Energy Physics - Vol.6 (1990) 61, "Quark Gluon Plasma" (Edt. R.C. Hwa), Singapore 1990, World Scientific. World Scientific, Singapore.
- [3] C. DeTar, *Quark-Gluon Plasma in Numerical Simulations of Lattice QCD*, UUHEP-95-2, to appear in "Quark Gluon Plasma 2" (Edt. R.C. Hwa), World Scientific.
- [4] K. Kanaya, Finite Temperature QCD on the Lattice, UTHEP-325.
- [5] A. Linde, Phys. Lett. 96B (1980) 289.
- [6] P. Arnold and C.-X. Zhai, Phys. Rev. D50 (1994) 7603;  
C.-X. Zhai and B. Kastening, *The free energy of hot gauge theories with fermions through  $g^5$* , PURD-TH-95-03.
- [7] U.M. Heller, F. Karsch and J. Rank, Phys. Lett. B355 (1995) 511.
- [8] G. Bali, J. Fingberg, U.M. Heller, F. Karsch, and K. Schilling, Phys. Rev. Lett. 71 (1993) 3059.
- [9] F. Karsch, E. Laermann and M. Lütgemeier, Phys. Lett. B 346 (1995) 94.
- [10] J. Engels, F. Karsch and K. Redlich, Nucl. Phys. B 435 (1995) 295.
- [11] B. Beinlich, F. Karsch and E. Laermann, *Improved Actions for QCD Thermodynamics on the Lattice*, BI-TP 95/33.
- [12] G. Boyd, J. Engels, F. Karsch, E. Laermann, C. Legeland, M. Lütgemeier and B. Petersson, Phys. Rev. Lett. 75 (1995) 4169.
- [13] J. Fingberg, U. Heller and F. Karsch, Nucl. Phys. B 392 (1993) 493.
- [14] Y. Iwasaki, K. Kanaya, T. Yoshié, T. Hoshino, T. Shirakawa, Y. Oyanagi, S. Ichii and T. Kawai, Phys. Rev. D 46 (1992) 4657.
- [15] S.A. Gottlieb, J. Kuti, D. Toussaint, A.D. Kennedy, S. Meyer, B.J. Pendleton and R.L. Sugar, Phys. Rev. Lett. 55 (1985) 1958;  
N.H. Christ and A.E. Terrano, Phys. Rev. Lett. 56 (1986) 111.
- [16] J. Engels, J. Fingberg, F. Karsch, D. Miller and M. Weber, Phys. Lett. B 252 (1990) 625.
- [17] H. Leutwyler, in Proceedings of the Conference *QCD - 20 years later*, (Edts. P.M. Zerwas and H.A. Kastrup), World Scientific 1993, p. 693.
- [18] T. Blum, L. Kärkkäinen, D. Toussaint and S. Gottlieb, Phys. Rev. D51 (1995) 5153.
- [19] for a review and further references see for instance: M.A. Shifman in *QCD 20 years later, Vol. 2*, ed. P.M. Zerwas and H.A. Kastrup (World Scientific, Singapore 1993).
- [20] R. Pisarski and F. Wilczek, Phys. Rev. D29 (1984) 339.

- [21] F. Wilczek, Intern. J. Mod. Phys. A7 (1992) 3911;  
K. Rajagopal and F. Wilczek, Nucl. Phys. B399 (1993) 395.
- [22] E. Shuryak, Comments Nucl. Part. Phys. 21 (1994) 235.
- [23] A. Kocić and J. Kogut, Phys. Rev. Lett. 74 (1995) 3109.
- [24] F. Karsch, Phys. Rev. D49 (1994) 3791.
- [25] F. Karsch and E. Laermann, Phys. Rev. D50 (1994) 6954.
- [26] for a recent Monte Carlo evaluation of  $O(4)$  exponents and further references see: K. Kanaya and S. Kaya, Phys. Rev. D51 (1995) 2404.
- [27] C. DeTar and J.B. Kogut, Phys. Rev. D36 (1987) 2828;  
K.D. Born et al., Phys. Rev. Lett. 67 (1991) 302.
- [28] G. Boyd, S. Gupta, F. Karsch, E. Laermann, B. Petersson and K. Redlich, Phys. Lett. B349 (1995) 170.
- [29] V.L. Eletsky and B.L. Ioffe, Phys. Rev. D47 (1993) 3083.
- [30] F. Karsch, Z. Phys. C38 (1988) 147;  
D.H. Rischke, M.I. Gorenstein, A. Schäfer, H. Stöcker, and W. Greiner, Phys. Lett. B278 (1992) 19;  
V. Goloviznin and H. Satz, Z. Phys. C57 (1993) 671;  
A. Peshier, B. Kämpfer, O.P. Pavlenko and G. Soff, Phys. Lett. B337 (1994)